Electron Paramagnetic Resonance Study of the Migratory Ant *Pachycondyla marginata* abdomens

E. Wajnberg,* D. Acosta-Avalos,* L. J. El-Jaick,* L. Abraçado,* J. L. A. Coelho,* A. F. Bakuzis,[†] P. C. Morais,[†] and D. M. S. Esquivel*

*Centro Brasileiro de Pesquisas Físicas, Rio de Janeiro (RJ), 20290-180, and [†]Universidade de Brasília, Instituto de Física, Núcleo de Física Aplicada, 70910-900, Brasília (DF), Brazil

ABSTRACT　Electron paramagnetic resonance was used to investigate the magnetic material present in abdomens of *Pachycondyla marginata* ants. A $g \cong 4.3$ resonance of high-spin ferric ions and a very narrow $g \cong 2$ line are observed. Two principal resonance broad lines, one with $g > 4.5$ (LF) and the other in the region of $g \cong 2$ (HF), were associated with the biomineralization process. The resonance field shift between these two lines, HF and LF, associated with magnetic nanoparticles indicates the presence of cluster structures containing on average three single units of magnetite-based nanoparticles. Analysis of the temperature dependence of the HF resonance linewidths supports the model picture of isolated magnetite nanostructures of ~13 nm in diameter with a magnetic energy of 544 K. These particles are shown to present a superparamagnetic behavior at room temperature. The use of these superparamagnetic particle properties for the magnetoreception process of the ants is suggested.

INTRODUCTION

Biomineralized magnetic materials have been studied since the early 1960s, when magnetite was identified in chiton teeth (Lowenstam, 1962). Among the biomineralized magnetic materials, magnetite is the most common (Lowenstam and Kirschvink, 1985), being widely produced in organisms from bacteria (Blakemore, 1975) to human beings (Kirschvink et al., 1992, Schultheiss-Grassi et al., 1999). Although magnetic orientation of living beings is a very complex phenomenon and the biological mechanism for detecting the geomagnetic field is still poorly understood, biomineralized magnetite seems to be a good candidate for the hypothesis of magnetic particle receptors. The geomagnetic field exerts a strong influence upon some species of insects (Wiltschko and Wiltschko, 1995). The most studied one has been the honeybee *Apis mellifera*, the abdomen of which presents magnetic nanoparticles with diameters in the range of 30–35 nm (Gould et al., 1980). The influence of geomagnetic field changes on the behavior of ants has been studied in the species *Solenopsis invicta* (Anderson and Vander Meer, 1993), *Formica rufa* (Çamlitepe and Stradling, 1995), and *Oecophylla smaragdina* (Jander and Jander, 1998). Investigations of abdomen tissues of *S. invicta* confirm the presence of ferrous iron (Slowick and Thorvilson, 1996). An interesting model for the study of the magnetoreception phenomenon is that of migratory insects, as in the case of the monarch butterfly, *Danaus plexippus* (Perez et al., 1999). Another migratory insect species is the ant *Pachycondyla marginata*, which has very peculiar habits: a diet of living termites and migration in a preferential direction (Leal and Oliveira, 1995). These habits make such a migratory ant very attractive for the study of biomineralized magnetic materials. Physical techniques such as magnetometry and high-resolution electron microscopy (Kirschvink et al., 1992, Bazylinski et al., 1994) have traditionally been used to investigate biomineralized magnetite in living beings. Magnetic resonance studies have shown the presence of magnetic material in *S. invicta* that is possibly related to magnetite (Esquivel et al., 1999). One of the main issues, as far as the physical techniques are concerned, is to establish a methodology that enables one to identify the different magnetic structures in unknown or biomineralized magnetic systems, such as magnetic material in living beings. For this purpose, magnetic resonance emerges as a very promising technique because it is sensitive enough to probe very small amounts of inorganic precursors, as well as of biomineralized magnetic material, in addition to the size and shape dependence of the resonance spectra on the nanometric magnetic structures. In this work, we used magnetic resonance to investigate the magnetic nanoparticles present in the abdomen of *Pachycondyla marginata*.

MATERIALS AND METHODS

Pachycondyla marginata ants were collected in the region of Campinas, São Paulo, Brazil. The ants were extensively washed with 80% ethanol and conserved in this solution. Abdomens of ~100 individuals were taken, dried for half an hour at ~70°C, and macerated. The resulting powder was transferred to the quartz electron paramagnetic resonance (EPR) tubes and sealed under nitrogen flux. The measurements were performed in a commercial X-band EPR spectrometer (Bruker ESP300E) operating at a microwave power of 4 mW with a modulation field ~2 Oe in amplitude.

RESULTS AND DISCUSSION

Fig. 1 shows typical EPR spectra as a function of temperature from 3 to 288 K. It is first noticed that there is a single
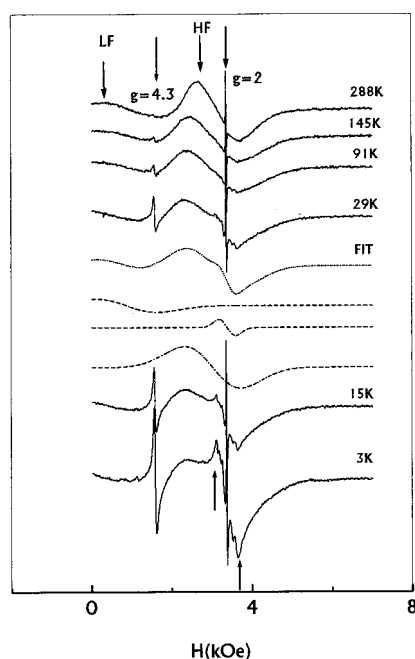
FIGURE 1 Typical X-band resonance spectra of *P. marginata* abdomens at different temperatures. The dotted line is the fit of the spectrum at 29 K, using the three Gaussian components given by the dashed lines.

sharp asymmetrical line at $g = 4.3$, characteristic of magnetically isolated high spin $S = 5/2$ Fe^{3+} ions in a low-symmetry environment. The high $g = 4.3$ factor has been attributed to the presence of relatively strong crystalline fields due to the lack of a crystal structure, typical of very small agglomerates containing ferric ions (Yahiaoui et al., 1994). The sharp resonance line close to $g = 2$ is assumed to be related to free radicals resulting from biological processes (Knowles et al., 1976). Nevertheless, similar results were observed in heat-treated glasses with a low iron doping level, which present a two-line pattern consisting of a narrow and a broad line at $g = 2$ (Berger et al., 1997). They were assumed to arise from small and large superparamagnetic particles, respectively. With an increase in the heat treatment temperature, the intensity of the narrow component decreases, as the latter is converted into the broad component, the intensity of which increases. The contribution of a nanoparticle precursor to the narrow line can also be considered.

From now on the broad resonance line around $g = 2$ will be referred to as the high-field (HF) resonance line. Another broad magnetic resonance structure is identified in the spectra at high g values and will be referred to as the low-field (LF) resonance line. At this point it must be noted that the LF line also has a strong correlation with the HF line. As is common in magnetic resonance experiments, it is recognized that while the HF line must be due to single magnetic nanoparticles, the LF line must be due to a chain or aggregate of those nanoparticles (Sharma and Waldner, 1977;

Fanin et al., 1993; Dorman et al., 1997). From the resonance point of view, the signature of the correlation between the single-like and the cluster-like magnetic structures is the fact that the temperature dependence of the resonance field of both broad resonance lines generates curves almost parallel to each other in a wide range of temperatures. A final comment concerning the spectra shown in Fig. 1 is the presence of an extra resonance structure appearing at low temperatures and superimposed to the HF line. Its intensity increases when the temperature decreases to 3 K. It presents a manganese-like structure, as has been previously observed in other ant species (Krebs and Benson, 1965). It is clearly observed at 3 K, as indicated by the two arrows at the peaks. Differently from the HF and the LF lines, this extra structure shows no shift in the resonance field as the temperature decreases to 3 K. This temperature behavior indicates that this spectral component is related to another structure, independent of the magnetic ones with the LF and HF features.

The following analysis will be focused on the two broad resonance lines, namely the LF line ($\sim$1.1 kOe) and the HF line ($\sim$3.1 kOe). The two broad lines (LF and HF) were fitted using Gaussian-shaped curves to obtain the temperature dependence of both the resonance linewidth (ΔH_R) and the resonance field (H_R). For temperatures lower than 100 K a third Gaussian line was considered to account for the extra resonance structure that appears at lower temperatures. The dotted line in Fig. 1 is a typical fit, using the three Gaussian components (*dashed lines*). Figs. 2 and 3 show, respectively, the resonance linewidth and resonance field associated with the two broad resonance lines as a function of temperature. The data shown in Figs. 2 and 3 are partially explained, as long as we assume that two distinct magnetite-based structures are present in the sample, namely, the isolated nanoparticles (INPs) and clustered nanoparticles (CNPs), associated, respectively, with the HF and LF resonance lines. Magnetite was chosen because it is the most common magnetic iron oxide found in living beings (Wiltschko and Wiltschko, 1995). Ferritin and hemosiderin are proteins with a superparamagnetic core of ferric hydroxide (Mann et al., 1989), which could also be the origin of HF and LF features. Although there have been no EPR studies on these ant proteins, human ferritin and hemosiderin EPR spectra also present two features called A and B. However, their intensity ratio is different from the ratio between the LF and HF structures. Moreover, the temperature behaviors shown in this study are not those described for those proteins (Weir et al., 1985). The proteins are then ruled out as the origin of the observed spectra. Above 70 K, the temperature dependence of the HF resonance linewidth follows the characteristic behavior of isolated magnetic nanoparticles (Morais et al., 1987). Below 70 K, however, the temperature dependence of the HF resonance linewidth deviates remarkably from the isolated nanoparticle picture. Furthermore, it is observed that the temperature dependence
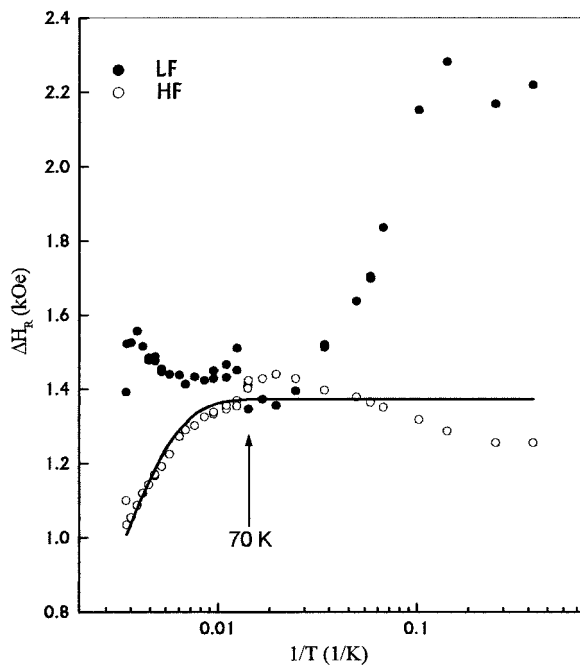
FIGURE 2 Temperature dependence of the resonance linewidth of the two broad resonance lines (HF and LF). The solid line is the best fit of the HF data above 70 K according to Eq. 1, with $\Delta H_R^0 = 1373 \pm 10$ Oe and $\Delta E = 272 \pm 7$ K.
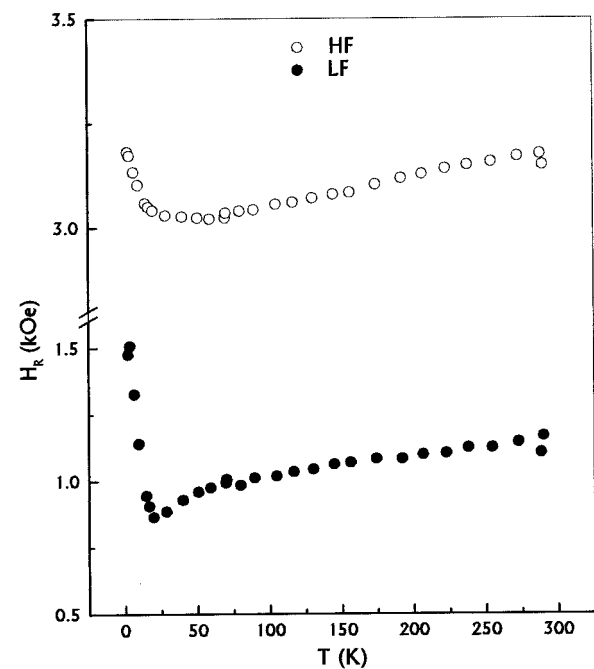

FIGURE 3 Temperature dependence of the resonance field of the two broad resonance lines (HF and LF). Note that above 70 K the two curves are almost parallel to each other, with the field shifted by 2033 ± 13 Oe.

of the resonance linewidth of the LF and HF lines shows clear opposite tendencies (Fig. 2). Such a difference could be due to the presence of two distinct magnetic structures (INPs and CNPs). On the other hand, except for a shift on the order of 2 kOe, the resonance fields of the LF and HF lines show very similar temperature dependences (Fig. 3). Above 70 K the temperature dependences of the resonance fields (LF and HF) show a linear-like behavior running almost parallel to each other, and the HF resonance linewidth is in very good agreement with the picture of an ensemble of isolated magnetic nanoparticles dispersed in a nonmagnetic matrix. Within this picture the approximate description of the resonance linewidth broadening is expressed by (Morais et al., 1987)

$$\Delta H_R = \Delta H_R^0 \tanh(\Delta E/2k_B T) \qquad (1)$$

where $\Delta H_R^0 = 5g\beta Sn/D^3$ and $\Delta E = KV$ is mainly associated with the magnetic anisotropy energy barrier height, where K is the magnetic anisotropy and V is the particle volume. The description of the prefactor ΔH_R^0 in Eq. 1 includes the g factor (g), the Bohr magneton (β), the spin associated with each magnetic center inside the nanoparticle (S), the number of magnetic centers per particle (n), and the particle-particle distance in the matrix (D). The solid line in Fig. 2 shows that the HF linewidth data fit nicely with Eq. 1 at temperatures above 70 K, in excellent agreement with the picture of isolated magnetic nanoparticles. The fitted parameters related to the solid line in Fig. 2 are $\Delta H_R^0 = 1373 \pm 10$ Oe

and $\Delta E/2k = 272 \pm 7$ K. Note that the prefactor (1373 ± 10 Oe) was fitted with no assumption concerning the particular values of g, S, n, and D. However, such a value is not far from the value we find (1350 Oe), assuming $g = 2$, $S = 2$, $n = 2 \times 10^4$, and $D = 14$ nm. $S = 2$ is reasonable for magnetite, because the octahedral and tetrahedral Fe^{3+} spins cancel each other while the eight octahedral Fe^{2+} respond for the net magnetization of the unit cell, presenting a $3d^6$ configuration. $n = 2 \times 10^4$ corresponds to a magnetite particle ~14 nm in diameter. As shown below, the average value estimated for the particle diameter in the INP structure is ~13 nm. These two average values, namely, 14 nm for the particle-particle distance and 13 nm for the particle diameter, are quite reasonable and indicate that nanomagnetite particles are not magnetically coupled together in the INP structure, although they are very close to one another. The sample preparation may pin the nanomagnetic particles to the host dielectric matrix. As a matter of fact, values for ΔH_R^0 of a few hundreds of Oe have been found in ferrite-based nanomagnetic particles dispersed as magnetic fluids (Morais et al., 1997). Indeed, no particular distribution function was used to describe the particle size polydispersity therefore the parameters associated with the solid line in Fig. 2 represent just average values. Although ferric particle size distributions have been observed by electron microscopy in the abdomens of ants (Acosta-Avalos et al., 1999), they are not adequate for our purposes, because they are expected to be distinct from those of EPR smashed samples,

where the magnetic particles are inside intact biological structures (Moskowitz et al., 1988).

To explain the temperature dependence of the resonance field in both HF and LF resonance lines, the resonance frequency ω_R, i.e., the Larmor precession frequency of the particle magnetic moment in the presence of an effective magnetic field (H_{EFF}), is considered:

$$\omega_R = \gamma H_{EFF} \quad (2)$$

where γ is the gyromagnetic ratio. As in traditional EPR experiments, the magnetic field strength is scanned instead of the microwave frequency, which is fixed. Thus the effective field is a result of three main components: the external sweeping field (H_E), the demagnetizing field (H_D), and the anisotropy field (H_A). At the resonance condition H_E corresponds to the resonance field H_R. In general, the calculation of H_{EFF} is extremely complicated, although a simple expression could be obtained as long as some initial considerations were taken into account (Vonsovskii, 1966). Considering the INP system as composed of spherical nanoparticles, the resonance field is given by (Vonsovskii, 1966)

$$H_R = \omega_R/\gamma - H_A \quad (3)$$

In contrast, assuming the CNP system to be composed of a linear chain of spheres, the picture of a prolate ellipsoid is fairly adequate to describe the system. In addition, assuming the prolate ellipsoid to be uniformly magnetized, the field inside the ellipsoid is known as the demagnetizing field (H_D) and can be written in terms of the demagnetizing perpendicular ($N_\perp$) and parallel ($N_\parallel$) tensor components, namely $H_D = (N_\perp - N_\parallel)M_S$. If the parallel axis corresponds to the easy magnetic axis of the particle, the resonance field can be written as follows (Vonsovskii, 1966; Kittel, 1996):

$$H_R = \omega_R/\gamma - (N_\perp - N_\parallel)M_S - H_A \quad (4)$$

where $(N_\perp - N_\parallel) > 0$ and M_S is the saturation magnetization associated with the magnetic nanoparticle. Inspection of Eqs. 3 and 4 reveals that the temperature dependence of the resonance field is mainly associated with the last term on the right-hand side (H_A), through its dependence on the magnetic anisotropy. If the two systems (INP and CNP) have the same anisotropy field behavior, then the resonance field associated with them would have the same temperature dependence, presenting curves parallel to each other and shifted by $(N_\perp - N_\parallel)M_S$. Above 70 K an average shift of 2033 ± 13 Oe between the two H_R versus T curves is obtained (Fig. 3). From this shift in field and assuming a linear chain of spherical nanoparticles for the CNP structure it is possible to estimate the average number of units in the chain (q). An ellipsoid of revolution, characterized by three principal axes (a, b, and c) such that $a \gg b = c$, is assumed in the calculation of the parallel component of the demagnetizing tensor ($N_\parallel$). Within this picture (Vonsovskii, 1966)

we have

$$N_\parallel = 4\pi\{q \ln[q + (q^2 - 1)^{1/2}]/(q^2 - 1)^{1/2} - 1\}/(q^2 - 1)$$

It is assumed that $b = c$ and that these are equal to the average value of the nanoparticle diameter, whereas the longer axis (a) is given by an integer times this diameter. Therefore, the dimensional ratio q is given by $q = a/b$. To calculate $N_\perp$ we make use of $N_\parallel + 2N_\perp = 4\pi$. Assuming the saturation magnetization value of bulk magnetite to be 470 Oe, a calculated field shift of 1994 Oe matches $q = 3$ ($N_\parallel = 1.3666$ and $N_\perp = 5.600$), suggesting a linear chain of three nanoparticles in average for the CNP structure. Using Eqs. 3 and 4 for the resonance field and the parameters $\nu = 9.445 \times 10^9$ Hz and $\gamma = 2.21 \times 10^5$ Hz·m/A ($g = 2.0$), the anisotropy field H_A is obtained; this is shown in Fig. 4. The anisotropy field in spherical magnetite nanoparticles is due to the effective magnetocrystalline anisotropy density (K_{EFF}) and is given by $H_A = 2K_{EFF}/M_S$. In magnetic nanoparticles the effective anisotropy energy density has both bulk (K_B) and surface (K_S) components; the bulk and surface components are temperature dependent, and the latter is related to the surface-to-volume ratio (Dimitrov and Wysin, 1994). In particular, the magnetocrystalline anisotropy in ferrite-based materials is usually discussed in terms of a single-ion contribution associated with the Fe^{3+} ion (Yosida and Tachiki, 1957). In general, K_{EFF} and M_S are both temperature dependent. However, considering that our data were taken in a temperature range far below the Curie temperature for bulk magnetite (850 K), M_S could be taken
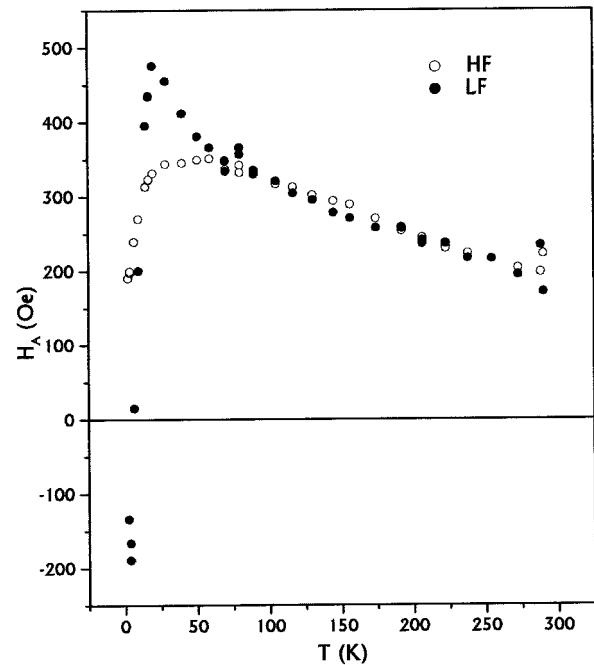

FIGURE 4 Anisotropy fields calculated from the resonant fields values, using Eqs. 3 and 4 for the HF and LF lines, respectively.

as approximately flat. Therefore, the temperature dependence of the anisotropy field would follow mainly the temperature dependence of the effective magnetic anisotropy. From data above 70 K, a mean value of $(6.4 \pm 0.4) \times 10^4$ erg/cm^3 was estimated for K_{EFF}. Using this value and the ΔE value from the linewidth analysis, an average magnetic volume of $(1.2 \pm 0.1) \times 10^3$ nm^3 was found, corresponding to a diameter of 13 ± 0.4 nm. A first approach to treating the data quantitatively (shown in Fig. 4) would be to employ mean-field theory (Millev and Fähnle, 1995). As long as the magnetite nanoparticle is assumed to be uniaxial, the free energy can be expressed in terms of two phenomenological anisotropy parameters, which in turn can be calculated from a generation function written in terms of the spin value and the magnetization. A relatively simple generation function can be obtained in the case of $S \leq 2$. In this case the data shown in Fig. 4 are in good agreement with this theory at temperatures above 70 K. Below 70 K, however, results obtained with the aforementioned approach deviate remarkably from the experimental data, indicating that a more complicated behavior takes place.

These EPR measurements in biological magnetic nanoparticles have allowed us to identify two different structures in ant abdomens: isolated nanoparticles with a diameter of ~13 nm and clusters that may be a linear chain of three particles. It is worth mentioning that this model is not restricted to chains or aggregates and can be applied to any nonspherical particles as revolution ellipsoids.

This volume estimated for the isolated particle is lower than that obtained by electron microscopy, through which were estimated the most probable length (20 nm) and width (16 nm) (Acosta-Avalos et al., 1999). However, the volume calculated is not the actual volume of the particle but the magnetic volume, and it depends on the physical principles of the measuring technique. Magnetic resonance in ferro (ferri)-magnetic nanoparticles could be considered a collective phenomenon, in which the magnetic resonance of the total magnetic moment of the nanoparticle is driven by the resonance of each magnetic sublattice in the nanoparticle.

The loss of magnetic order is related to surface effects that weaken the exchange interaction near the surface (Kodama et al., 1996; Martínez et al., 1998), disorienting the surface spins and reducing the effective volume that can be involved in magnetic resonance. It is possible that collective disorder may generate randomness in the exchange interactions deep in the nanoparticle, reducing even more the effective volume measured by magnetic resonance. The temperature dependence of surface effects (Martínez et al., 1998) may be related to the anomalous behavior observed in this study at temperatures lower than ~70 K.

It is interesting to remark that the magnetic volume experimentally calculated for ants is lower than the magnetic volume estimated for honeybees (Gould et al., 1980). However, the great variety of living beings that present magnetic nanoparticles ensures the size diversity of those nanoparticles, because they must be related to specialized cells, the sizes of which must vary with the kind of organism considered.

Magnetite nanoparticles with a diameter of ~13 nm are superparamagnetic at room temperature. A magnetic energy $\Delta E/k = 544$ K (even 1632 K for the three-particle chain) yields a relaxation time on the order of nanoseconds at room temperature (Néel, 1949). Intensity changes of magnetic fields seem to provoke oscillations in the neuron frequency pattern of honeybees only after some minutes of stimulation. Sometimes the response becomes strongly oscillatory, with periods similar to the stimulus periods of the order of seconds (Schiff, 1991). The relaxation time is then very short as compared to the neurological response times in honeybees and reinforces the superparamagnetic character. It was suggested that in honeybees, superparamagnetic magnetite is involved in gradient detection by locally amplifying changes in the geomagnetic field (Schiff and Canal, 1993). Similar to other social insects such as bees, ants could take advantage of the almost instantaneous response of superparamagnetic particles to a magnetic intensity gradient involved in a map sense orientation (Schiff, 1991). More recently (Shcherbakov and Winklhofer, 1999) it was proposed that magnetic-field-induced shape change of a cluster of magnetite nanoparticles could be amplified as well as counterbalanced by osmotic pressure. This mechanism could play an important role in magnetoreception. Both models are based on the existence of magnetoreceptors, here characterized for migratory ants. Regardless of the relevance of characterizing the magnetic receptor candidates, only behavioral experiments can actually confirm their use in magnetic orientation.

REFERENCES

Acosta-Avalos, D., E. Wajnberg, P. S. Oliveira, I. Leal, M. Farina, and D. M. S. Esquivel. 1999. Isolation of magnetic nanoparticles from *Pachycondyla marginata* ants. *J. Exp. Biol.* 202:2687–2692.

Anderson, J. B., and R. K. Vander Meer. 1993. Magnetic orientation in the fire ant, *Solenopsis invicta. Naturwissenschaften.* 80:568–570.

Bazylinski, D. A., A. J. Garrattreed, and R. B. Frankel. 1994. Electron microscopy studies of magnetosomes in magnetotactic bacteria. *Microsc. Res. Tech.* 27:389–401.

Berger, R., J. C. Bissey, J. Kliava, and B. Soulard. 1997. Superparamagnetic resonance of ferric ions in devitrified borate glass. *J. Magn. Magn. Mater.* 167:129–135.

Blakemore, F. 1975. Magnetotactic bacteria. *Science.* 19:377–379.

Çamlitepe, Y., and D. J. Stradling. 1995. Wood ants orient to magnetic fields. *Proc. R. Soc. Lond. B.* 261:37–41.

Dimitrov, D. A., and G. M. Wysin. 1994. Effects of surface anisotropy on hysteresis in fine magnetic particles. *Phys. Rev. B.* 50:3077–3084.

Dorman, J. L., D. Fiorani, and E. Tronc. 1997. Magnetic relaxation in fine-particle systems. *In* Advances in Chemical Physics, Vol. XCVIII. I. Prigogine and S. A. Rice, editors. John Wiley and Sons, New York. 283–494.

Esquivel, D. M. S., D. Acosta-Avalos, L. J. El-Jaick, A. D. M. Cunha, M. G. Malheiros, E. Wajnberg, and M. P. Linhares. 1999. Evidence for magnetic material in the fire ant *Solenopsis sp.* by electron paramagnetic resonance measurements. *Naturwissenschaften.* 86:30–32.

Fanin, P. C., B. K. P. Scaife, and S. W. Charles. 1993. Relaxation and resonance in ferrofluids. *J. Magn. Magn. Mater.* 122:159–163.

Gould, J. L., J. L. Kirschvink, K. S. Deffeyes, and M. L. Brines. 1980. Orientation of demagnetized bees. *J. Exp. Biol.* 86:1–8.

Jander, R., and U. Jander. 1998. The light and magnetic compass of the weaver ant, *Oecophylla smaragdina* (Hymenoptera: Formicidae). *Ethology.* 104:743–758.

Kirschvink, J. L., Kobayashi-Kirschvink, A., and B. J. Woodford. 1992. Magnetite biomineralization in the human brain. *Proc. Natl. Acad. Sci. USA.* 89:7683–7687.

Kittel, C. 1996. Introduction to Solid State Physics. John Wiley, New York.

Knowles, P. F., D. Marsh, and H. W. E. Rattle. 1976. Magnetic Resonance of Biomolecules. Wiley, London.

Kodama, R. H., A. E. Berkowitz, E. J. McNiff, Jr., and S. Foner. 1996. Surface spin disorder in $NiFe_2O_4$ nanoparticles. *Phys. Rev. Lett.* 77: 394–397.

Krebs, A. T., and B. W. Benson. 1965. Electron spin resonance in Formicidae. *Nature.* 207:1410–1413.

Leal, I. R., and P. S. Oliveira. 1995. Behavioral ecology of the neotropical termite hunting ant *Pachycondyla marginata*—colony founding, group-raiding and migratory patterns. *Behav. Ecol. Sociobiol.* 37:373–383.

Lowenstam, H. A. 1962. Magnetite in denticle capping in recent chitons (polyplacophora). *Geol. Soc. Am. Bull.* 73:435–438.

Lowenstam, H. A., and J. L. Kirschvink. 1985. Magnetic Biomineralization and Magnetoreception in Organisms. Plenum Press, New York.

Mann, S., J. Webb, and R. J. P. Williams, editors. 1989. Biomineralization: Chemical and Biochemical Perspectives. VCH Publishers, New York.

Martínez, B., X. Obradors, L. Balcells, A. Rouanet, and C. Monty. 1998. Low temperature surface spin-glass transition in γ-Fe_2O_3 nanoparticles. *Phys. Rev. Lett.* 80:181–184.

Millev, Y., and M. Fähnle. 1995. Types of temperature dependence of single-ion magnetic anisotropy constants by general thermodynamic considerations. *Phys. Rev. B.* 52:4336–4352.

Morais, P. C., M. C. F. L. Lara, and K. Skeff Neto. 1987. Electron spin resonance in superparamagnetic particles dispersed in a non-magnetic matrix. *Philos. Mag. Lett.* 55:181–183.

Morais, P. C., A. L. Tronconi, F. A. Tourinho, and F. Pelegrini. 1997. Investigation of the Brownian relaxation and hydrodynamic radius in nanomagnetic particles. *Solid. State Commun.* 101:693–697.

Moskowitz, B. M., R. B. Frankel, P. J. Flanders, R. P. Blakemore, and B. B. Schwartz. 1988. Magnetic properties of magnetotactic bacteria. *J. Magn. Magn. Mater.* 73:273–288.

Néel, L. 1949. Théorie du traînage magnétique des ferromagnétique en grains fins avec applications aux terres cuites. *Ann. Geophys.* 5:99–136.

Perez, S. M., O. R. Taylor, and R. Jander. 1999. The effect of a strong magnetic field on monarch butterfly (*Danaus plexippus*) migratory behavior. *Naturwissenschaften.* 86:140–143.

Schiff, H. 1991. Modulation of spike frequencies by varying the ambient magnetic field and magnetite candidates in bees (*Apis mellifera*). *Comp. Biochem. Physiol.* 100:975–985.

Schiff, H., and G. Canal. 1993. The magnetic and electric fields induced by superparamagnetic magnetite in honeybees. *Biol. Cybern.* 69:7–17

Schultheiss-Grassi, P. P., R. Wessiken, and J. Dobson. 1999. TEM investigation of biogenic magnetite extracted from the human hippocampus. *Biochem. Biophys. Acta.* 1426:212–216.

Sharma, V. K., and F. Waldner. 1977. Superparamagnetic and ferrimagnetic resonance of ultrafine Fe_3O_4 particles in ferrofluids. *J. Appl. Physiol.* 48:4298–4302.

Shcherbakov, V. P., and M. Winklhofer. 1999. The osmotic magnetometer: a new model for magnetite-based magnetoreceptors in animals. *Eur. Biophys. J.* 28:380–392.

Slowick, T. J., and H. G. Thorvilson. 1996. Localization of subcuticular iron-containing tissue in the red imported fire ant. *Southwest. Entomol.* 21:247–254.

Vonsovskii, S. V. 1966. Ferromagnetic Resonance. Pergamon Press, New York.

Weir, M. P., T. J. Peters, and J. F. Gibson. 1985. Electron spin resonance studies of splenic ferritin and hemosiderin. *Biochem Biophys. Acta.* 828:298–305.

Wiltschko, R., and W. Wiltschko. 1995. Magnetic Orientation in Animals. Springer Verlag, Berlin.

Yahiaoui, E. M., R. Berger, Y. Servant, J. Kliava, L. Cugunov, and A. Mednis. 1994. Electron paramagnetic resonance of Fe^{3+} ions in borate glass computer simulation. *J. Phys. Condens. Matter.* 6:9415–9428.

Yosida, K., and M. Tachiki. 1957. On the origin of magnetic anisotropy energy in ferrites. *Prog. Theor. Phys.* 17:331–359.